Knockdown of lncRNA *MALAT1* induces pyroptosis by regulating the miR-124/SIRT1 axis in cervical cancer cells

TIAN LIANG[1*], TONG LU[2*], WEIWEI JIA[3*], RUNZE LI[4], MIN JIANG[5], YU JIAO[5], YUCHEN WANG[5], SHANSHAN CONG[1], XINYAN JIANG[1], LINA DONG[1], YINGYU ZHOU[4,6], GUANGMEI ZHANG[1] and DAN XIAO[4,7]

[1]Department of Obstetrics and Gynaecology, The First Affiliated Hospital of Harbin Medical University, Harbin, Heilongjiang 150081; [2]College of Medical Technology, Qiqihar Medical University, Qiqihar, Heilongjiang 161006; [3]Department of Basic Medicine School, Qiqihar Medical University, Qiqihar, Heilongjiang 161006; [4]School of Medicine and Health, Harbin Institute of Technology, Harbin, Heilongjiang 150001; [5]Department of Psychiatry, Qiqihar Medical University, Qiqihar, Heilongjiang 161006; [6]National and Local Joint Engineering Laboratory for Synthesis Transformation and Separation of Extreme Environmental Nutrients, Harbin, Heilongjiang 150001; [7]Zhengzhou Research Institute, Harbin Institute of Technology, Zhengzhou, Henan 450007, P.R. China

Received January 7, 2021; Accepted August 20, 2021

DOI: 10.3892/ijo.2023.5586

Abstract. The aim of the present study was to elucidate the role and downstream mechanism of long non-coding RNA (lncRNA) metastasis-associated lung adenocarcinoma transcript 1 *(MALAT1)* in the process of cervical cancer cell pyroptosis. The effect of inhibiting lncRNA *MALAT1* on cervical cancer cells was determined using primary cells isolated from patients and U14 cervical tumor-bearing nude mice. The level of lncRNA *MALAT1* expression and cell viability were determined for relationship analysis. Pyroptosis was then investigated in HeLa cells with lncRNA *MALAT1* knockdown or overexpression with or without lipopolysaccharide (LPS) treatment. Bioinformatics tools were used to identify downstream factors of lncRNA *MALAT1*, which were subsequently verified by gain- or loss-of-function analyses in the process of cervical cancer cell pyroptosis. It was observed that the level of lncRNA *MALAT1* was markedly higher in cervical carcinoma cells compared with expression in paracarcinoma cells, and knockdown of lncRNA *MALAT1* induced cervical cancer cell death through pyroptosis. By contrast, overexpression of lncRNA *MALAT1* blocked LPS-induced pyroptosis. These results, combined with bioinformatics statistical tools, demonstrated that the microRNA (miR)-124/sirtuin 1 (SIRT1) axis may affect the progression of cervical cancer at least partly by mediating the effect of lncRNA *MALAT1* on the pyroptosis of cervical cancer cells. In conclusion, the lncRNA *MALAT1*/miR-124/SIRT1 regulatory axis in cervical cancer cells may mediate pyroptosis and may provide potential targets against the progression of cervical cancer.

Correspondence to: Dr Dan Xiao, School of Medicine and Health, Harbin Institute of Technology, 92 West Dazhi Street, Harbin, Heilongjiang 150001, P.R. China
E-mail: xiaodan5433@163.com

Professor Guangmei Zhang, Department of Obstetrics and Gynaecology, The First Affiliated Hospital of Harbin Medical University, 23 Youzheng Street, Harbin, Heilongjiang 150081, P.R. China
E-mail: guangmeizang@126.com

*Contributed equally

Key words: long non-coding RNA metastasis-associated lung adenocarcinoma transcript 1, microRNA-124, sirtuin 1, cervical carcinoma, pyroptosis

Introduction

Cervical carcinoma is the most malignant and life-threatening type of cancer in women. Indeed, as the fourth most common malignant tumor worldwide. According to the World Health Organization (WHO), in 2020, there were a total of 604,000 new cases and 342,000 deaths. In 2015, it was estimated that there were 111,000 new cases of cervical cancer in China, with an estimated death toll of ~ 33,800 individuals (1), highlighting the treatment of cervical cancer is of great importance (2,3), and research focused on its pathogenesis and therapeutic targets has generated interest in various fields (4).

Several programmed cell death mechanisms, such as apoptosis, have been investigated as important mechanisms of anticancer defense (4). However, the association between pyroptosis and cancer remains to be further clarified. Pyroptosis is a form of programmed cell death; morphological changes involve cells continuously expanding until the membrane ruptures, resulting in the release of cellular contents, which triggers a strong inflammatory response (5). The specific process of pyroptosis includes stimulation by pathogens, followed by recognition of these signals by intracellular NOD-like receptor (NLR) and activation of caspase-1 through the binding of the adaptor protein apoptosis-associated speck-like protein containing a caspase recruitment

domain (ASC) to pro-caspase-1 (6). Subsequently, activated caspase-1 cleaves gasdermin (GSDM) D, thus forming holes in cell membrane and releasing cellular contents, which eventually induces pyroptosis (7,8). In addition, pyroptosis is characterized by the production of activated IL-1β and IL-18, which are released to the extracellular space, causing an inflammatory response (9,10). The expression of NLR protein 3 (NLRP3)-related downstream molecules, including ASC, caspase-1, IL-1β and IL-18, in atherosclerotic plaques is significantly higher compared with that in non-atherosclerotic vessels; the upregulation of their expression levels is closely associated with plaque fragility, suggesting that pyroptosis activation mediates the evolution of atherosclerotic lesions (11). It has also been reported that pyroptosis may contribute to cancer prevention and treatment (12). A study exploring the mechanism of gastric cancer chemotherapy demonstrated that GSDME can convert chemotherapy-induced apoptosis into pyroptosis to achieve therapeutic purposes (13). Additionally, α-naphthoyl-ethyltrimethylammonium represents a potential novel antitumor molecule, as it has been reported to induce pyroptosis of epithelial ovarian cancer cells (14). Based on these studies, it appears that pyroptosis may be of value in the treatment of cancer.

Comprehensive treatment of cervical cancer is mainly based on surgery and radiotherapy, supplemented by chemotherapy in clinical practice (15). Considering the fertility requirements, drug tolerance and side effects of traditional treatments, novel strategies against cervical cancer require further studies on potential molecular targets. Long non-coding RNAs (lncRNAs) are a class of RNA molecules with transcripts >200 nucleotide in length that are usually involved in protein-coding gene regulation at the epigenetic, transcriptional and post-transcriptional levels. Numerous lncRNAs have been reported to be involved in several physiological and pathological mechanisms, particularly malignant tumorigenesis (16). For example, lncRNA plasmacytoma variant translocation 1 is closely associated with myelocytomatosis progression and may represent a therapeutic target (17). lncRNA metastasis-associated lung adenocarcinoma transcript 1 *(MALAT1)* was initially recognized in non-small cell lung cancer (NSCLC) and is one of the most studied lncRNAs in cancer owing to its high abundance and conservation. For example, *MALAT1* suppresses breast cancer metastasis by targeting TEA domain family members (18). In addition, lncRNA *MALAT1* can promote tumorigenesis in colorectal, ovarian and gallbladder cancer (19-21). In addition, lncRNA *MALAT1* was shown to regulate downstream microRNAs (miRNAs/miRs) by binding complementary sequences, including miR-129-5p, and the miR-129-5p/high mobility group box protein 1 axis, during colon cancer development (22), miR-200a during lung cancer cell proliferation (23) and miR-124, and the miR-124/calpain small subunit 1 axis, in nasopharyngeal carcinoma (24). Although lncRNA *MALAT1* serves a crucial role in regulating cancer progression, including cell proliferation, invasion (19) and epithelial-to-mesenchymal transition (25), limited research has been conducted on the role of lncRNA *MALAT1* in pyroptosis (26), particularly on cervical tumorigenesis. The present study hypothesized that lncRNA *MALAT1* is the key mediator on pyroptosis during cervical cancer, regulating tumor progression. The present study aimed to elucidate the potential mechanism underlying lncRNA *MALAT1* during cervical cancer and to offer important insights into pyroptosis.

Materials and methods

Human subjects. A total of 11 patients (age, 48-62 years) with newly diagnosed cervical carcinoma, who received treatment at the First Affiliated Hospital of Harbin Medical University (Harbin, China) between January 2019 and August 2020, were enrolled in the present study. Ethical approval was obtained from the Ethics Committee of the First Affiliated Hospital of Harbin Medical University (approval no. IRB-AF/SC-04/02.0; 11 November 2020); tumor samples were collected from the patients upon written informed consent. Human carcinoma and paracarcinoma tissues (1-5 cm away from carcinoma tissue) were collected for the culture of isolated primary cells.

Animals. The experimental protocols involving animals were approved by the Animal Ethical Care Committee of Qiqihar Medical University (Qiqihar, China; approval no. QMU-AECC-2020-43; 8 May 2020) and complied with the Guide for the Use and Care of Laboratory Animals published by the USA National Institutes of Health (NIH Publication No. 85-23, revised 1996) (27). BALB/c nude female mice (n=10; age, 6 weeks; weight, 18-22 g) were provided by the Animal Center of Qiqihar Medical University and were housed in a dedicated room with a 12-h dark/light cycle, controlled temperature (22±1˚C) and constant humidity (55±5%); mice had free access to a standard diet and water. After 1 week of acclimatization, $2x10^6$ U14 mouse cervical carcinoma cells (BeNa Culture Collection; Beijing Beina Chunglian Institute of Biotechnology) were intraperitoneally (i.p.) injected in the C57BL/6 mice to prepare the U14 ascites tumor cells; cells were allowed to grow for 7 days, ensuring the abdominal ascites did not exceed 20% body weight (endpoint weight, 20.3-24.2 g). The abdominal ascites were collected as follows: i) Mice were anesthetized with 150 mg/kg tribromoethanol i.p. (cat. no. M2910; Nanjing Aibei Biotechnology Co., Ltd.) until loss of corneal reflex, muscle tightness and response to skin pinch; ii) the abdomen was swabbed with 75% alcohol, a small incision was made in the center of the skin overlying the peritoneal wall and the skin was firmly pulled to expose the peritoneal wall; iii) i) a 25 G needle was inserted into the peritoneal membrane, avoiding inserting needle into intestine or bladder, and 5 ml saline was injected into the peritoneal cavity; iv) the abdomen was massaged for approximately 10-15 sec, then the needle was withdrawn slowly; v) using one hand, the fluid was pushed to one side of the peritoneum and, with the other hand, the needle was inserted into the side of cavity with plenty of fluid and as much of the fluid as possible was withdrawn from the peritoneum; vi) the needle was removed, the contents of the syringe were dispensed into a centrifuge tube on ice, which was then centrifuged at 4˚C, 183 x g for 5 min to collect cell pellet; vii) the U14 ascites tumor cells were resuspended and passaged for 10 days. The U14 cells were cultured in RPMI-1640 medium (Gibco; Thermo Fishers Scientific, Inc.) supplemented with 10% fetal bovine serum (FBS; Gibco; Thermo Fisher Scientific, Inc.) and 1% penicillin-streptomycin (Gibco; Thermo Fisher Scientific,

Inc.) at 37˚C in a humidified atmosphere containing 5% CO_2. Following collection of ascetic fluid the mice were euthanized with pentobarbital sodium (100 mg/kg; i.p.).

The U14 cervical cells were subsequently divided into two groups and transfected as follows: i) Short hairpin (sh)RNA negative control (sh-Control) and ii) shRNA against lncRNA *MALAT1* (sh-MALAT1). The effectiveness of transfection was confirmed as shown in Fig. S1. The tumor cell density was adjusted to $1x10^7$ cells/ml using normal saline. The right subaxillary skin of the mice was disinfected and inoculated with 0.2 ml U14 cervical cancer cell suspension for the establishment of 20 nude mice bearing U14 cervical tumor xenografts (n=10 mice/group). After 4 weeks, the maximum tumor diameter was 14 mm; tumors were excised after euthanasia using 100 mg/kg pentobarbital injection. The tumor volume was calculated as the follows: Tumor volume=(length x width^2)/2. The tumor index included tumor diameter (range, 0.7-1.4 cm), volume (range. 0.1-0.726 cm^3) and weight (range, 0.12-0.62 g).

Isolated primary cell culture. Carcinoma and paracarcinoma tissues were isolated from four patients with cervical cancer and prepared for culture according to the following steps: i) Tissue block was placed into a pre-cooled sterile culture medium on ice at room temperature for 5 min; ii) tissue was were washed at room temperature with non-FBS-containing DMEM for 3 times under and cut; iii) tissue was enzymatically dissociated by the addition of 0.05% trypsin-EDTA for overnight at 4˚C; iv) rinsed with 0.2% collagenase I for 10 min and collected the cell supernatant at room temperature v) repeated the step iv until none tissue coarse left; v) cell supernatant was filtered with 100 μm mesh filter and centrifuged at 183 x g for 10 min at 4˚C, and the supernatant was discarded; viii) the cell pellet was resuspended in fresh culture medium; and ix) cells were incubated overnight at 37˚C in a humidified air atmosphere containing 5% CO_2; x) Upon attainment of dense culture (after 2-3 weeks of primary culture), cells were passaged by mechanical dissociation via trituration with a Pasteur pipet, and transferred into separated culture medium containing plasks at room temperature (28). The culture medium used was DMEM with high glucose containing 5% FBS (Gibco; Thermo Fisher Scientific, Inc.), 1% antibiotics and HEPES (10 mM). The viability of primary cervical cancer cells was evaluated by trypan blue assay; the number of live cells was >70%.

HeLa cell culture. The HeLa cervical cancer cell line was obtained from Shanghai Institutes for Biological Sciences and was cultured in RPMI-1640 medium (Thermo Fisher Scientific, Inc.) supplied with 10% FBS and 1% penicillin/streptomycin (100 μg/ml) in 5% CO_2 at 37˚C.

Lipopolysaccharide (LPS) treatment. Before treatment, cells ($1x10^6$ cells/ml) were seeded and serum-starved with FBS-free restriction treatment medium overnight, according to the study by Qiu *et al* (29). LPS (Beijing Solarbio Science & Technology Co., Ltd.) dissolved in sterile deionized water was used at a final cell culture concentration of 1 μg/ml and cells were incubated for 24 h in 5% CO_2 at 37˚C (28).

Cell transfection. Isolated primary cervical carcinoma cells from human patients, U14 and HeLa cells were seeded into 6-well plates at a density of $2x10^6$ cells/well. When the confluence reached 80%, the cells were incubated in serum-free medium for 24 h before transfection. Transfection was performed using Lipofectamine™ 2000 (Invitrogen; Thermo Fisher Scientific, Inc.) according to the manufacturer's instructions. Lentiviral particles (Shanghai GenePharma Co., Ltd.) containing the specific shRNAs (100 nM) for sh-Control (5'-GGGUGA ACUCACGUCAGAA-3'), sh-MALAT1-1 (5'-CACAGGGAA AGCGAGUGGUUGGU-3') and sh-MALAT1-2) (5'-GAC AGGUAUCUCUUCGUUAUC-3') were transduced into the cells for 12 h, and fresh medium was then changed for subsequent 48 h culture in 5% CO_2 at 37˚C. The interference efficiency was detected by reverse transcription-quantitative PCR (RT-qPCR). Similarly, sirtuin 1 (SIRT1) shRNA (5'-TGC GGGAATCCAAAGGATAATTTTCAAGAGAAATTATCC TTTGGATTCCCGCTTTTTC-3') and sh-Control (5'-TGC AACAAGATGAAGAGCACCAATTCAAGAGATGGTGCT CTTCATCTTGTTGTTTTTTC-3') were also purchased from Shanghai GenePharma Co., Ltd. and used to transfect cells as aforementioned.

The MALAT1 overexpression plasmid (pcDNA3.1-MALAT1; NCBI accession: NR_002819.4, nucleotides 3,207-8,411 bp) was constructed as previously described (26,27). The MALAT1-vector plasmid and the empty vector plasmid were purchased from Shanghai GenePharma Co., Ltd. A total of 50 ng/ml plasmid was transfected into cells using Lipofectamine® 2000 Transfection Reagent (Beijing Solarbio Science & Technology Co., Ltd.) according to the manufacturer's instructions. miR-124 mimics (50 nM) and negative control (NC; 50 nM) were transfected into cells using X-treme GENE reagent (Invitrogen; Thermo Fisher Scientific, Inc.) at 37˚C. The sequences of the miR-124 mimics were as follows: Sense 5'-UAAGGCACGCGGUGA AUGCC-3' and anti-sense 5'-CAUUCACCGCGUGCC UUAUU-3'. The sequences of the negative controls were as follows: Sense 5'-UUCUCCGAACGUGUCACGUTT-3' and anti-sense 5'-ACGUGACACGUUCGGAGAATT-3'. After 6 h transfection, the medium was replaced with normal growth medium, and total RNA and protein were extracted at 24 h post-transfection.

RT-qPCR. Total RNA was extracted from cells using TRIzol® (Invitrogen; Thermo Fisher Scientific, Inc.). cDNA synthesis was performed using a High-Capacity cDNA Reverse Transcription Kit (Applied Biosystems; Thermo Fisher Scientific, Inc.) according to the manufacturer's instructions. The levels of lncRNA *MALAT1*, miR-124, *SIRT1*, *NLRP3*, caspase-1 and *ASC* were determined by the SYBR Green I (Roche Diagnostics) incorporation method using an ABI 7500 Fast Real-Time PCR System (Applied Biosystems; Thermo Fisher Scientific, Inc.). The thermocycling conditions were as follows: Initial denaturation for 30 sec at 95˚C; followed by 40 cycles of 5 sec at 95˚C and 30 sec at 60˚C. *GAPDH* was used as the internal control for lncRNA *MALAT1*, *SIRT1*, *NLRP3*, caspase-1 and *ASC*; *U6* was used as the internal control for miR-124. The primer sequences are shown in Table I. The relative expression levels were calculated using the $2^{-\Delta\Delta Cq}$ method (30).

Western blotting. Total protein for western blot analysis was extracted and dissolved in RIPA buffer (Beijing Solarbio

Table I. Primer sequences used for reverse transcription-quantitative PCR.

Gene	Primer sequence (5'→3')
lncRNA *MALAT1*	F: TGAGTCGAGCTCTGCCAAGTCC TGGAGAAATAGTAG
	R: AGTCATGGGCCCTGAAGACAG ATTAGTAAAAGCA
NLRP3	F: GAT CTTCGCTGCGATCAACA
	R: GGGATTCGAAACACGTGCATTA
Caspase-1	F: GCCTGTTCCTGTGATGT GGAG
	R: TGCCCACAGACATTCATACAGT TTC
ASC	F: CTGACGGATGAGCAGTACCA
	R: CAGATGATTTGGTGGGATT
SIRT1	F: GUAUUGCUGAACAGAUGGAUU
	R: UCCAUCUGUUCAGCAAUACUU
GAPDH	F: CCTGCACCACCAACTGCTTA
	R: -GGCCATCCACAGTCTT CTGAG
miRNA-124	F: UUAAGGCACGCGGUGAAUGC
	R: CAGTGCGTGTCGTGTCGTGGAT
U6	F: 5'-GCTTCGGCAGCACATATACTA AAAT
	R: 5'-CGCTTCACGAATTTGCGTGT CAT

ASC, apoptosis-associated speck-like protein containing a caspase recruitment domain; F, forward; lncRNA, long non-coding RNA; *MALAT1*, metastasis-associated lung adenocarcinoma transcript 1; *NLRP3*, NOD-like receptor protein 3; R, reverse; *SIRT1*, sirtuin 1.

Science & Technology Co., Ltd.) with protease inhibitors (Sigma-Aldrich; Merck KGaA). The BCA method (Beyotime Institute of Biotechnology) was used to quantify the protein concentration. Proteins (80 μg/15 μl into each well) were separated by 10% SDS-PAGE and then transferred to a nitrocellulose membrane. The membranes were blocked with 5% skimmed milk for 2 h at room temperature, then incubated with primary antibodies against SIRT1 (1:1,000, Abcam, Catalog No. ab110304), NLRP3 (dilution at 1:1,000, Abcam, Catalog No. ab263899), caspase-1 (dilution at 1:1,000, Abcam, Catalog No. ab207802), cleaved caspase-1 (dilution at 1:1,000, Cell Signaling Technology, Inc. Catalog No. 89332), ASC (dilution at 1:1,000, Abcam, Catalog No. ab283684) and GAPDH (dilution at 1:500, OriGene Technologies, Inc. Catalog No. TA802519) at 4˚C for 12 h. The membranes were then incubated with FITC-conjugated goat anti-rabbit (1:10,000, Invitrogen; Thermo Fisher Scientific, Inc. catalog No. A-11008) or goat anti-mouse secondary antibody (dilution at 1:10,000, Invitrogen; Thermo Fisher Scientific, Inc. Catalog No. A-11001) was incubated for 2 h at room temperature in the dark. Odyssey Infrared Imaging System (LI-COR Biosciences) and its analysis software (Odyssey version 3.0) were used to calculate the relative expression level compared with the internal control (GAPDH).

ELISA. IL-1β and IL-18 in cell culture medium were determined using Human IL-1β (Interleukin 1 Beta) ELISA Kit (Cat. No. E-EL-H0149) and Human IL-18 (Interleukin 18) ELISA Kit (Cat. No. E-EL-H0253), respectively, from Elabscience Biotechnology, Inc., following the manufacturer's instructions.

Immunofluorescence staining. Hela cells (seeding density of 70% were fixed with 4% paraformaldehyde solution (Beyotime Institute of Biotechnology) for 30 min at room temperature and permeabilized with 0.4% Triton X-100 (Beyotime Institute of Biotechnology; catalog No. P0096-100 ml) for 30 min at room temperature. After 2-h blocking with goat serum (Beyotime Institute of Biotechnology, Catalog No. C0265) at room temperature, cells were then incubated with anti-NLRP3 (1:100; Abcam, Catalog No. ab263899) antibody at 4˚C for 24 h followed by incubation with FITC-labeled goat anti-rabbit immunoglobulin G (1:500; Invitrogen; Thermo Fisher Scientific, Inc. Catalog No. A16118) in the dark for 2 h at room temperature. DAPI (1 μg/ml; Beyotime Institute of Biotechnology) was used for nuclear staining; cells were incubated at room temperature in the dark. Conventional fluorescence microscopy (Nikon Corporation) was used for image capturing, and images were analyzed at x200 magnification. Three complete and non-overlapping views were randomly selected, and the mean optical density under each view were measured as manufacture of Image-pro plus (version 6.0).

TUNEL staining assay. Cell death was assessed using a TUNEL assay kit (Beijing Solarbio Science & Technology Co., Ltd.) in accordance with the manufacturer's instructions. Cells were stained with DAPI for nuclear staining, and three complete and non-overlapping views were randomly selected for examination under an Olympus IX51 fluorescence microscope (Olympus Corporation) at x100 magnification.

Measurement of caspase activity. Cell lysate (200 ml) was used for caspase activity detection using Caspase-1 Activity Assay kit (cat. no. C1101; Beyotime Institute of Biotechnology), Caspase-4 Activity Assay kit (cat. no. C1121; Beyotime Institute of Biotechnology) and Caspase-5 Colorimetric Analysis kit (cat. no. 55R-1283; AmyJet Scientific Inc.). Briefly, cells were collected with 50 μl of ice-cold lysis buffer for 1 h. Then, caspase activities were detected by spectrophotometer at A405 nm according to the manufacturer's instructions.

Bioinformatics analysis. Online bioinformatics tools for lncRNAs, including LncACTdb (http://www.bio-bigdata.net/LncACTdb; version 3.0/Sep. 2021), NPInter (http://bigdata.ibp.ac.cn/npinter; version 4.0/Sep. 2019) and LncBase (http://www.microrna.gr/LncBase; version 3.0/2019) were used to predict putative target miRNAs of lncRNA *MALAT1*. A Venn diagram was used to search for targets withing the intersections among these databases. Bioinformatic tools for miRNAs and its potential mRNA targets were also used, including starBase (https://starbase.sysu.edu.cn/starbase2/index.php; version 2.0/Sep. 2013), TargetScan (http://www.targetscan.org; version 7.2/March 2018) and miRDB (http://mirdb.org/miRDB; version 6.0/June 2019).

For predicting the downstream target mRNAs of selected miRNAs, first a Venn diagram was used to identify possible

candidates among the aforementioned databases. Furthermore, a literature search of the PubMed database (PMID: 33040786; PMID: 29844574; PMID: 33061806; PMID: 32232409; PMID: 34369271) with the key words 'pyroptosis and cervical cancer' was used to review possible regulators reported in previous studies. Finally, SIRT1 from bioinformatic databases and literature searches was identified as a potential target of miR-124 and selected for further examination in the present study.

RNA immunoprecipitation (RIP). The binding of lncRNA *MALAT1* to NLRP3 was detected with a Magna RIP™ RNA-Binding Protein Immunoprecipitation kit (EMD Millipore corp., 17-700). Hela cells (1-3x10^7 cells from manufacture, were washed with pre-cooled PBS and lysed with RIPA lysis buffer (Beyotime Institute of Biotechnology) in an ice bath for 5 min. The supernatant was collected after centrifugation at 20,000 x g for 10 min at 4˚C. An aliquot of the cell extract was used as the input. Cell extract was incubated with rabbit antibody against NLRP3 (1:100; Abcam) at room temperature for 30 min for co-precipitation. A rabbit anti-human IgG (cat. no. ab109489; 1:100; Abcam) was used as the negative control with a volume of 1 ml at room temperature for 30 min. Samples were shaken to the bottom and placed on a magnetic seat in an ice bath, and the supernatant was discarded after 1 min. Then, 1 ml NT-2 was added and the beads were shaken vigorously to mix. After 5-time centrifugate (5,000 x g, 15 sec at 4˚C) and washing with RIP Wash Buffer, the precipitate was collected and used as the sample. RNA was extracted after digestion by proteinase K at 55˚C for subsequent analysis. lncRNA *MALAT1* content in immunoprecipitated RNA was quantified by RT-qPCR and present as relative RNA level compared with IgG IP.

Cell morphology. After transfection and/or LPS treatment, HeLa cells were incubated for 24 h in a standard CO_2 incubator, and images were obtained with an inverted phase contrast microscope (Olympus Corporation) to observe and record the morphology of the cells.

Cell viability assay. Primary isolated cervical carcinoma cells from human patients (10^4 cells/well) and HeLa cells (10^4 cells/well) were seeded in a 96-well plate. After 24 h transfection and/or LPS treatment, Cell Counting Kit-8 reagent (Nanjing Jiancheng Bioengineering Institute) was added each well (10 μl/well) and incubated for 4 h at 37˚C. The optical density value at 450 nm was determined with a Bio-Rad 680 microplate reader (Bio-Rad Laboratories, Inc.).

Cell counting assay. Trypan blue staining (Beijing Solarbio Science & Technology Co., Ltd.) was used for cell counting. Primary isolated cervical carcinoma cells (and Hela cells (both 1x10^6 cells/ml) were resuspended and mixed with 0.1% trypan blue at room temperature for 5 min. Cells were counted using a Countless II FL automated cell counter (Invitrogen; Thermo Fisher Scientific, Inc.) and the ratio of living cells vs. dead cells was analyzed.

Statistical analysis. Data were analyzed using GraphPad Prism 5.0 software (GraphPad Software, Inc.). Data are presented as the mean ± standard error of the mean. All experiments were repeated three times. Statistical comparisons between two groups were performed by Student's t-test (paired t-test for the matched sample data and unpaired t-test for comparisons of two groups). One- or two-way ANOVA followed by Tukey's post hoc test was used for multiple comparisons. Association analyses were assessed by the linear regression index (r^2) (31). $P<0.05$ was considered to indicate a statistically significant difference.

Results

lncRNA MALAT1 is positively related with cervical tumor growth and negatively associated with cell death. To clarify the function of lncRNA *MALAT1* in cervical carcinoma, insight into its biological process from Gene Ontology (GO) analysis was gained by LncACTdb database. The top two GO term enrichment for lncRNA *MALAT1* are 'regulation of cell proliferation' and 'regulation of cell cycle' (Fig. 1A), which may be associated with cervical tumor progression. Thus, the present study aimed to determine the effect of lncRNA *MALAT1* on cervical cancer cell viability. Initially, primary cells were isolated from paracarcinoma and carcinoma tissues of patients with cervical cancer and cultures were established to compare the differential expression of lncRNA *MALAT1 in vitro*. The expression level of lncRNA *MALAT1* was significantly increased in cervical carcinoma cells compared with the paracarcinoma cells (Fig. 1B). Additionally, a positive association was found between lncRNA *MALAT1* levels and cell viability, as well as with live cell number, whereas the opposite was observed with the number of dead cells (Fig. 1C and D). These results suggested that lncRNA *MALAT1* is positively associated with cervical cancer cell viability, and the loss of lncRNA *MALAT1* may exert an inhibitory effect on the development of cervical cancer. To demonstrate this hypothesis, lncRNA *MALAT1* was knocked down with sh-*MALAT1* in isolated primary cervical carcinoma cells and in U14 cervical cancer cells (Fig. S1A and B, respectively). Knockdown of lncRNA *MALAT1* induced a marked increase in primary cervical carcinoma cell death *in vitro* (Fig. 1E) and also led to a decrease in *in vivo* tumor diameter, volume, and weight (Fig. 1F-H). These results suggested that specific knockdown of lncRNA *MALAT1* may function as a suppressor of cervical cancer cells through mechanisms that remain to be identified.

In addition, lncRNA *MALAT1* was overexpressed in isolated primary cervical carcinoma cells for in-depth exploration *in vitro* (Fig. S1C). Increased lncRNA *MALAT1* expression promoted cell viability of cervical cancer cells with no significant change in cell deaths (Fig. S2), which suggested the potential of lncRNA *MALAT1* overexpression on promoting cervical cancer growth.

Subsequent *in vitro* experiments were performed to further investigate the aforementioned effect of MALAT1 knockdown on cell death in HeLa cells (Fig. S1D). After transfection with sh-MALAT1, HeLa cervical cancer cells exhibited an increase in the number of TUNEL-positive cells (Fig. 2A and B) and increased levels of IL-18 and IL-1β in the culture medium (Fig. 2C). Thus, it was hypothesized that pyroptosis may have occurred in HeLa cells following knockdown of lncRNA *MALAT1* expression. Thus, the present study examined the

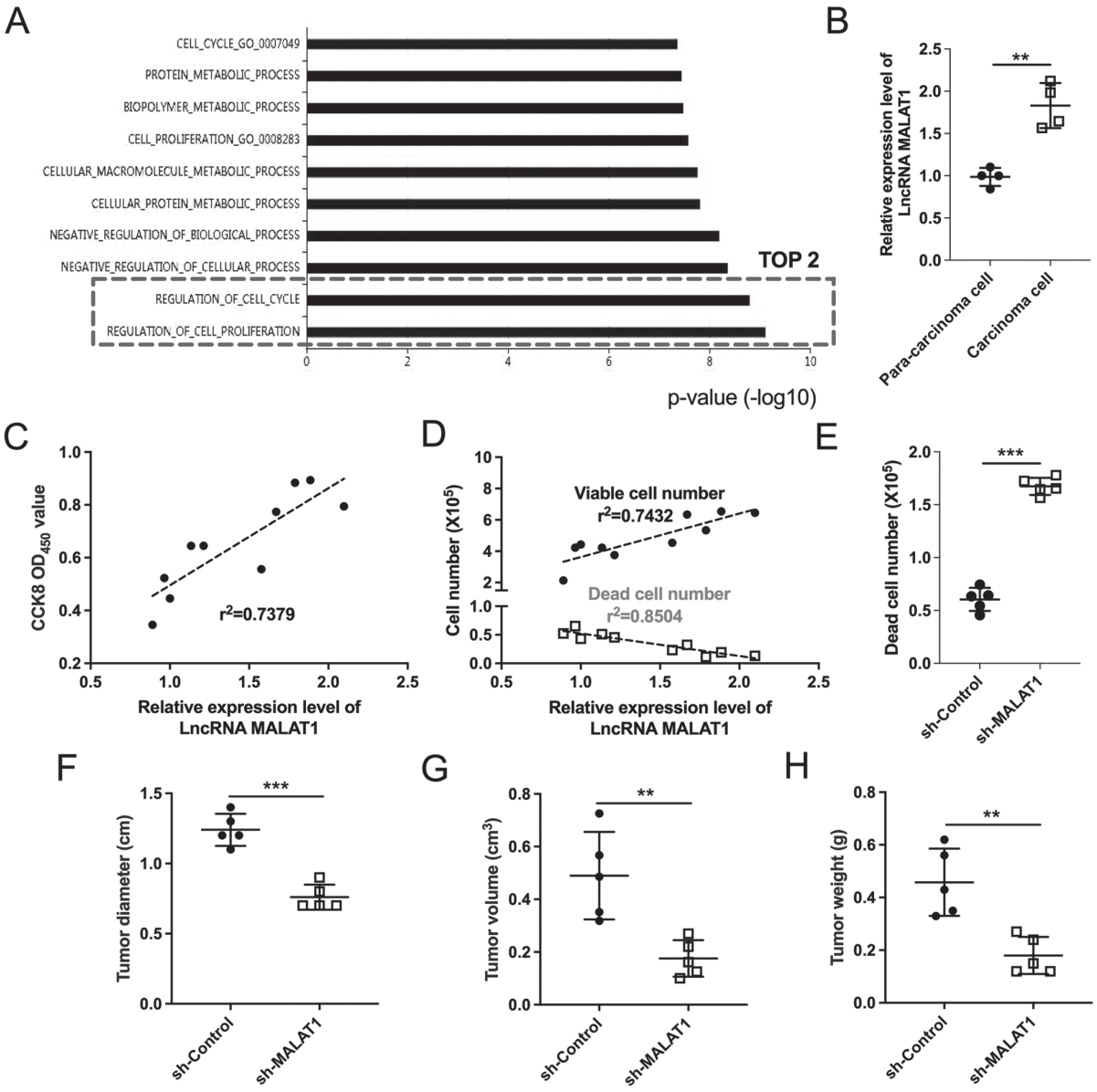

Figure 1. LncRNA *MALAT1* expression is associated with cervical cancer progression. (A) Gene Ontology analysis identified the top 10 biological processes associated with lncRNA *MALAT1*. (B) lncRNA *MALAT1* expression levels in primary cells isolated from paracarcinoma and carcinoma tissues were determined by reverse transcription-quantitative PCR. n=4 tissue samples/group; ***P<0.001. (C-E) Primary cells were isolated from human cervical carcinoma tissues and examined for viability and cell death. (C) Cell viability was determined by CCK-8 assay (n=10). (D) Viable and dead cell numbers were determined by trypan blue staining assay (n=10). (E) Number of dead cells was determined in the sh-Control and sh-MALAT1 transfection groups. n=5; ***P<0.001. (F) Tumor diameter (range, 0.7-1.4 cm), (G) volume (range, 0.1-0.726 cm^3) and (H) weight (range, 0.12-0.62 g) were determined in each group. n=5 mice/group; **P<0.01, ***P<0.001. CCK-8, Cell Counting Kit-8; lncRNA, long non-coding RNA; *MALAT1*, metastasis-associated lung adenocarcinoma transcript 1; OD, optical density; sh, short hairpin.

activity of pyroptosis-related caspases, the expression levels of NLRP3, caspase-1 and ASC, and examined changes in cell morphology following sh-MALAT1 transfection. It was observed that downregulated lncRNA *MALAT1* markedly increased caspase-1 activity (Fig. 2D), increased protein (Fig. 2E and F) and mRNA (Fig. 2G) expression levels of NLRP3, cleaved caspase-1 and ASC (Fig. 2E-G), and increased the number of cells exhibiting morphological evidence of membrane rupture (Fig. 2H). These changes may eventually lead cervical cancer cells to undergo pyroptosis.

Taken together, these results indicated that the reduction of lncRNA *MALAT1* expression may inhibit cervical cancer cell viability by inducing pyroptosis.

Overexpression of lncRNA MALAT1 protects HeLa cells from LPS-induced pyroptosis. To explore the effects of lncRNA *MALAT1* on cervical cancer cells against pyroptosis, lncRNA *MALAT1* was overexpressed in LPS-treated HeLa cells; confirmation of successful overexpression vector transfection was first confirmed in untreated HeLa cells (Fig. S1E). LPS treatment is generally used as a pyroptosis stimulus, which induces typical pyroptotic characteristics, including cell morphology (inflammasome-mediated membrane holes and cell swelling), decreased cell viability and increased levels of inflammatory factors (IL-1β and IL-18), as well as increased expression levels of NLRP3, cleaved caspase-1 and ASC upregulation according to previous studies (29,30). In the current study,

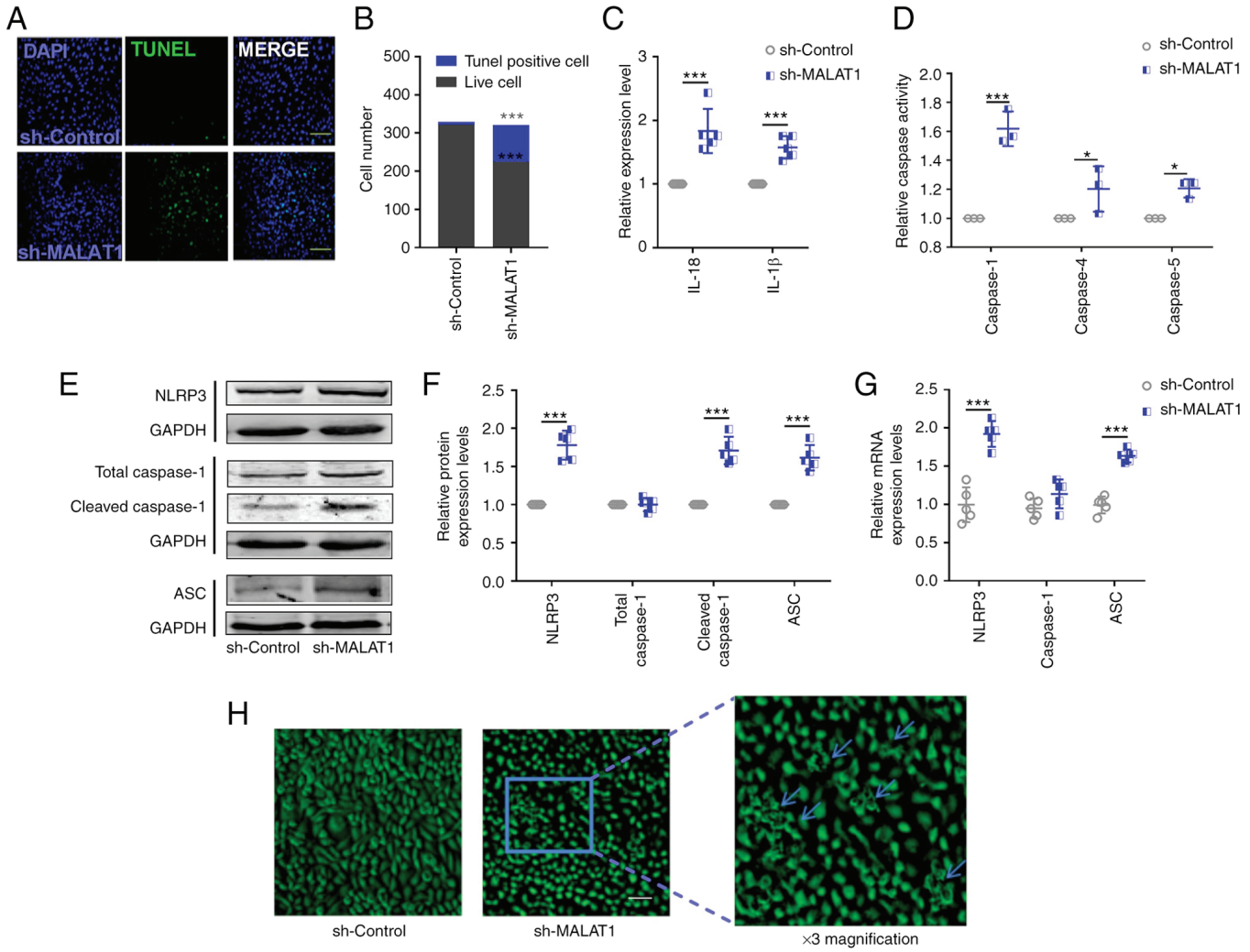

Figure 2. Downregulation of lncRNA *MALAT1* induces the pyroptosis of HeLa cervical cancer cells. (A) Representative images of the TUNEL-staining assay (scale bar, 50 μm) and (B) statistical analysis was performed to detect the number of living and dead cells. n=3; ***P<0.001. (C) ELISA kits were used to determine the levels of IL-18 and IL-1β in the culture medium of transfected HeLa cells. n=5; ***P<0.001. (D) The activities of caspase-1, caspase-4 and caspase-5 were determined with a caspase assay kit. n=3; *P<0.05, ***P<0.001. (E and F) Protein and (G) mRNA expression levels of pyroptosis-related factors, NLRP3, caspase 1 and ASC, were determined by western blotting and reverse transcription-quantitative PCR, respectively. n=5; ***P<0.001. (H) Cell morphology was observed by inverted phase contrast microscopy; blue arrows show the morphological changes. Scale bar, 50 μm; three-fold magnification is shown on the right. ASC, apoptosis-associated speck-like protein containing a caspase recruitment domain; *MALAT1*, metastasis-associated lung adenocarcinoma transcript 1; NLRP3, NOD-like receptor protein 3.

lncRNA *MALAT1* was overexpressed in LPS-treated cells, which led to a noticeable decrease in the number of swollen cells (Fig. 3A), an increase in HeLa cell viability (Fig. 3B) and downregulated levels of IL-1β and IL-18 (Fig. 3C), in addition to decreased protein expression levels of NLRP3, cleaved caspase-1 and ASC (Fig. 3D-F). The results suggested that lncRNA *MALAT1* may block the development of pyroptosis in LPS-treated HeLa cells.

Based on these data, it was concluded that lncRNA *MALAT1* may affect the progression of cervical cancer, at least in part through the regulation of pyroptosis. However, the mechanism by which lncRNA *MALAT1* initiates pyroptosis remains unclear, including whether lncRNA *MALAT1* directly interacts with pyroptotic factors, such as NLRP3, or interferes with them at the post-transcriptional level. NLRP3 is generally recognized to initiate pyroptosis (31), thus, it was proposed that lncRNA *MALAT1* may directly affect the expression of NLRP3 as a transcriptional factor. Immunofluorescent staining of NLRP3 showed a downregulated expression in *MALAT1* overexpressed cell under the condition of LPS treatment (Fig. 3G and H). RIP assays were performed in HeLa cells to verify whether there is a direct interaction between lncRNA *MALAT1* and NLRP3. Unexpectedly, no significant difference was identified in the RIP analysis for an lncRNA *MALAT1*/NLRP3 regulatory axis (Fig. 3I).

lncRNA MALAT1 affects the miR-124/SIRT1 axis in LPS-treated cervical cancer cells. To explore the downstream target of lncRNA *MALAT1* in regulating the pyroptotic process in cervical cancer cells, bioinformatics tools, Venn diagrams and literature searches using the key words 'pyroptosis and cervical cancer' were used. According to the results from three bioinformatics predictive databases (LncACTdb, NPInter and LncBase) and a Venn diagram, which was used to search for the intersection among the results of these databases, five potential targets of lncRNA *MALAT1* were identified,

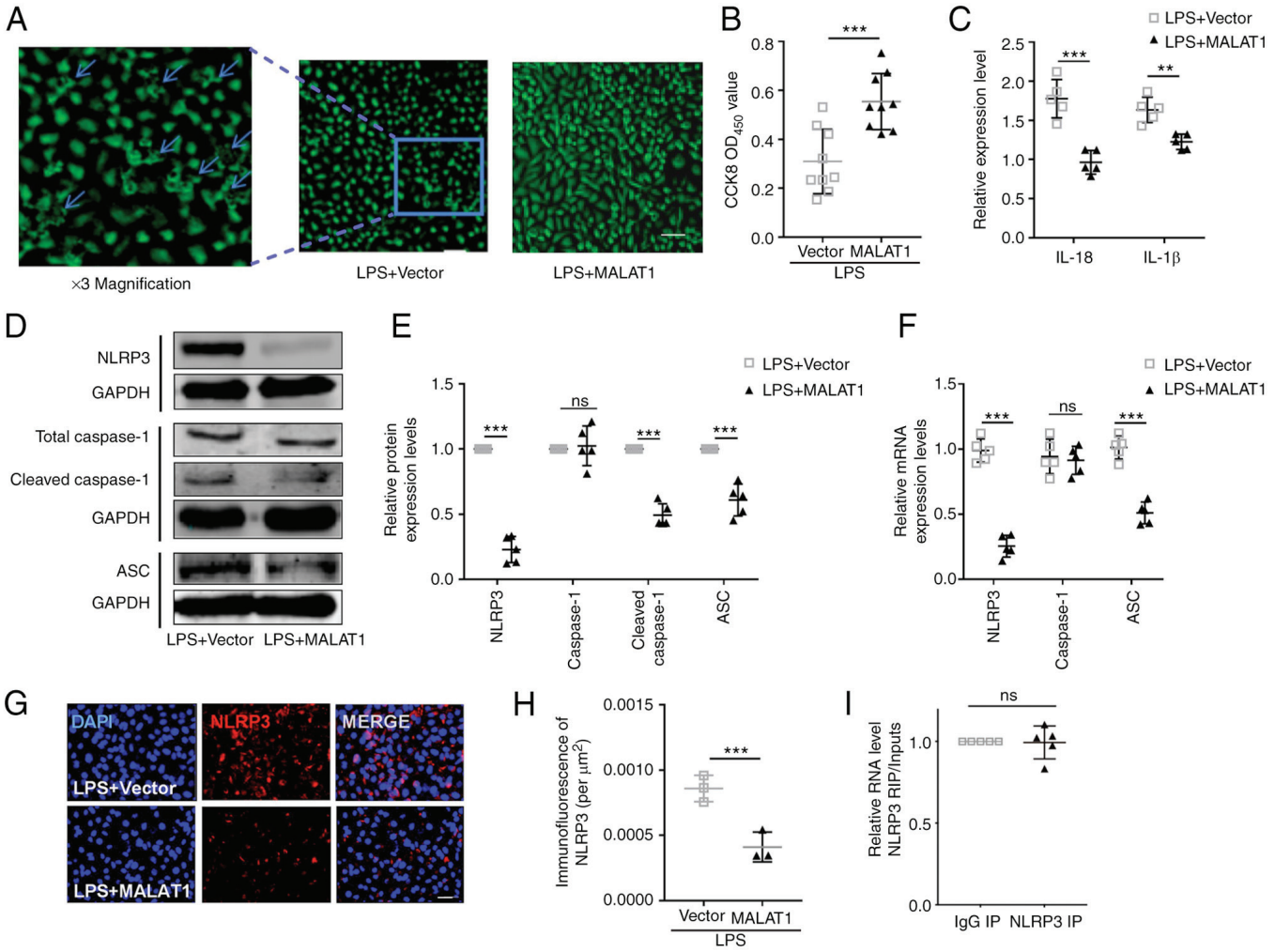

Figure 3. Upregulation of lncRNA *MALAT1* blocks the effect of LPS on HeLa cervical cancer cell pyroptosis. (A) Morphological changes (blue arrows) in Hela cells were used to assess cell pyroptosis by phase contrast microscopy. Scale bar, 50 μm Three-fold magnification is shown on the left for better clarification. (B) Hela cell viability was determined by CCK-8 assay. n=5; ***P<0.001. (C) ELISA kits were used to determine the levels of IL-18 and IL-1β in the culture medium. n=5; **P<0.01, ***P<0.001. (D and E) Protein and (F) mRNA expression levels of pyroptotic factors, including NLRP3, caspase-1 and ASC, were detected by western blotting and reverse transcription-quantitative PCR, respectively. n=5; **P<0.01, ***P<0.001. (G) Representative images and (H) statistical analysis of NLRP3 immunofluorescence; scale bar, 20 μm. n=5; ***P<0.001. (I) RNA immunoprecipitation analysis was used to determine the regulatory association between lncRNA *MALAT1* and NLRP3; n=3. ASC, apoptosis-associated speck-like protein containing a caspase recruitment domain; CCK-8, Cell Counting Kit-8; IP, immunoprecipitation; lncRNA, long non-coding RNA; LPS, lipopolysaccharide; *MALAT1*, metastasis-associated lung adenocarcinoma transcript 1; NLRP3, NOD-like receptor protein 3; ns, not significant; OD, optical density.

including miR-25-3p, miR-92b-3p, miR96-5p, miR-124 and miR-1 (Fig. 4A).

RT-qPCR was then performed to determine miRNA expression levels and to investigate if these molecules serve a role in lncRNA *MALAT1*-regulated pyroptosis in HeLa cells. The level of miR-124 exhibited the most significant alteration after LPS treatment (Fig. 4B); in addition, knockdown and overexpression of lncRNA *MALAT1* resulted in significant increase and decrease of miR-124 expression levels, respectively (Fig. 4C). These data suggested that miR-124 may be a downstream target of lncRNA *MALAT1*, particularly in pyroptosis.

Apart from lncRNA *MALAT1*, other putative targets of miR-124 were investigated; three bioinformatics prediction tools (starBase, TargetScan and miRDB) were used alongside a Venn diagram. A total of 82 potential targets of miR-124 were identified with the result of PubMed database search (using the key words 'pyroptosis and cervical cancer'). A previous study demonstrated the involvement of SIRT1 during pyroptosis, suggesting SIRT1 could therefore be a target for the effective treatment of cervical cancer (32) (Fig. S3A). Therefore, *SIRT1* was selected as a potential target of miR-124 (Fig. S3).

miR-124/SIRT1 mediates the effect of lncRNA MALAT1 on pyroptotic progression of HeLa cervical cancer cells. To investigate the potential target of lncRNA *MALAT1* during pyroptosis, subsequent experiments were divided into two parts: i) Verification the direct interaction between miR-124 and *SIRT1*, and ii) *SIRT1* mediating the function of lncRNA *MALAT1* in LPS-treated HeLa cells.

For the first part, the aim was to verify whether miR-124 mediated the effects of lncRNA *MALAT1* on pyroptosis. Thus, cells were co-transfected with lncRNA *MALAT1* overexpression vector with miR-124 mimics, attempting to disturb the function of lncRNA *MALAT1*. After the determination of transfection efficiency of miR-124 mimics in non-treated

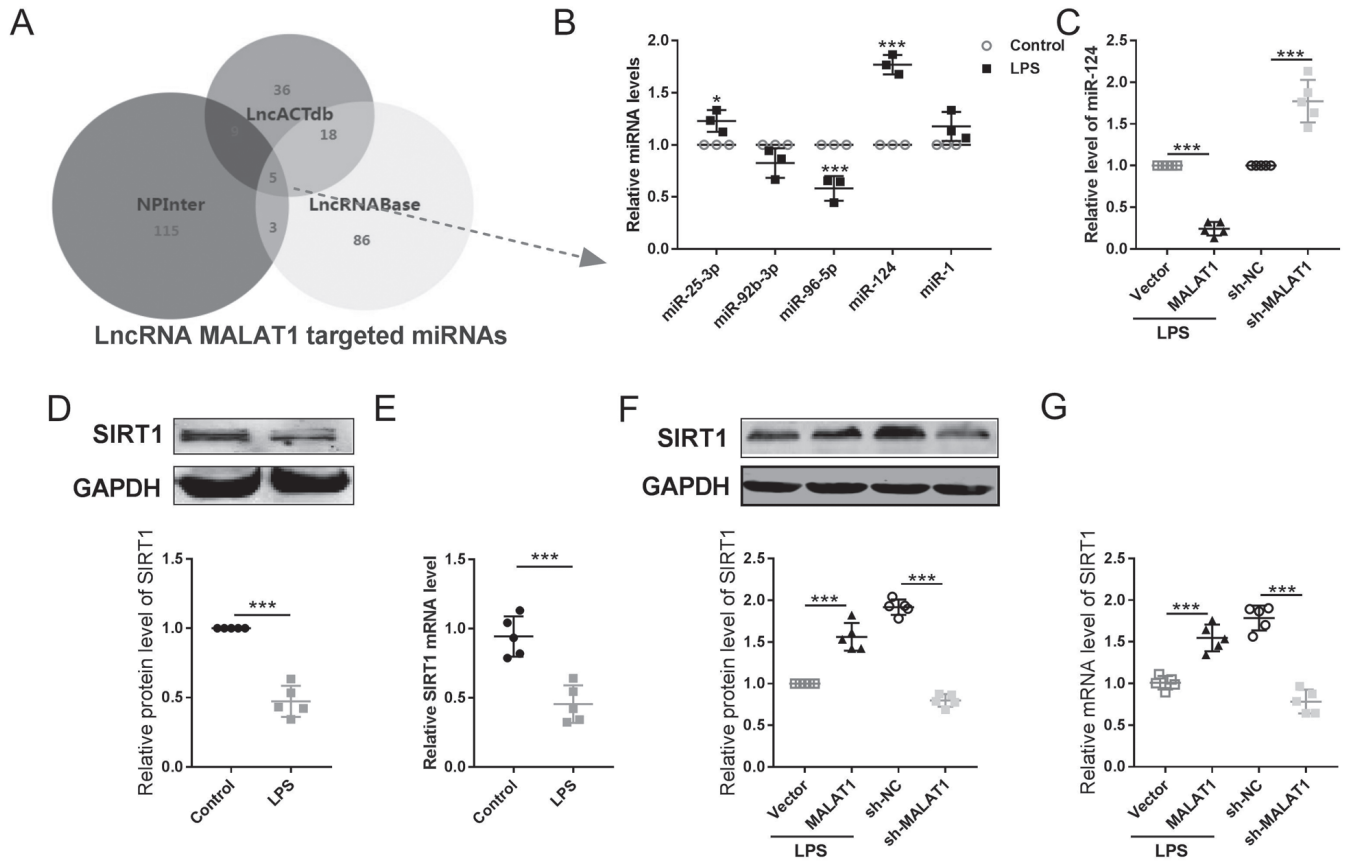

Figure 4. lncRNA *MALAT1* alters the expression levels of miR-124/SIRT1 in cervical tumor cell during pyroptosis. (A) Bioinformatics prediction analyses (LncACTdb, NPInter and LncRNABase) of lncRNAs and a Venn diagram were used to identify the possible downstream miRNA targets of lncRNA *MALATA1*. (B) Expression levels of the five miRNA candidates identified from the intersection of (A) were then detected by RT-qPCR in HeLa cells treated with or without LPS. n=5; *P<0.05, ***P<0.001. (C) The levels of miR-124 was determined by RT-qPCR. n=5; ***P<0.001. The expression levels of SIRT1 (D) protein and (E) mRNA were detected by western blotting and RT-qPCR, respectively. n=5; ***P<0.001. The expression levels of SIRT1 (F) protein and (G) mRNA were detected by western blotting and RT-qPCR, respectively. n=5; ***P<0.001. lncRNA, long non-coding RNA; LPS, lipopolysaccharide; *MALAT1*, metastasis-associated lung adenocarcinoma transcript 1; miR/miRNA, microRNA; RT-qPCR, reverse transcription-quantitative PCR; SIRT1, sirtuin 1.

HeLa cells (Fig. S4) and lncRNA *MALAT1* co-transfected HeLa cells (Fig. 5A), overexpression of miR-124, compared to its NC group, led to a decrease in the level of lncRNA *MALAT1* expression (Fig. 5B). Additionally, the overexpression of miR-124 also concurrently decreased the activity of HeLa cells (Fig. 5C). Our previous findings suggested that lncRNA *MALAT1* could 'protect' HeLa cells against pyroptotic damage induced by LPS. However, in this context, we discovered that miR-124 counteracted this ability of lncRNA *MALAT1*, evidenced by a subsequent increase in the expression of inflammatory factors IL-1β and IL-18 (Fig. 5D), promoted death of HeLa cells, and reduced number of viable HeLa cells (Fig. 5E and F). Further examination of pyroptotic factors NLRP3, ASC, and cleaved caspase 1 confirmed that miR-124 inhibited lncRNA *MALAT1*'s ability to protect HeLa cells against pyroptosis induced by LPS stimulation (Fig. 5G-I).

For the second part, experiments were conducted to verify whether SIRT1 underlies the function of lncRNA *MALAT1* on pyroptosis. HeLa cells were co-transfected with lncRNA *MALAT1* overexpression vector and sh-SIRT1 or its NC (Figs. S5A and 5B). Transfection of sh-SIRT1 functioned as an antagonist against lncRNA *MALAT1*, abolishing the protective effects of lncRNA *MALAT1* in HeLa cells from LPS, including reducing viable HeLa cells (Fig. 6C and D), increasing death number of HeLa cells (Fig. 6E). Transfection of sh-SIRT1 elevated inflammatory factors IL-1β and IL-18 (Fig. 6F) and pyroptotic factors NLRP3, ASC, and cleaved caspase 1 (Fig. 6G-I). Taken together, these results demonstrated the regulatory effect of the lncRNA *MALAT1*/miR-124/SIRT1 axis on cervical cancer cell pyroptosis.

Discussion

Although improvements have been made in terms of cervical cancer treatment (33), cervical cancer treatments face several challenges that limit their efficiency. Cervical cancer is primarily caused by infection with high-risk subtypes of the human papillomavirus (HPV). Although it is a preventable disease, limited resources, especially in low- and middle-income countries (LMICs) often lead to advanced and untreatable disease at the time of diagnosis. Early-stage detection is associated with significantly improved survival rates. However, screening programs may not be well-established, leading to delayed diagnosis and treatment initiation (34). The cost of cervical cancer treatment can be a significant burden for patients, even for those with insurance (35); 4) Recurrent cervical cancer remains challenging to treat, with poor prognosis and low overall survival rates (36). Despite these

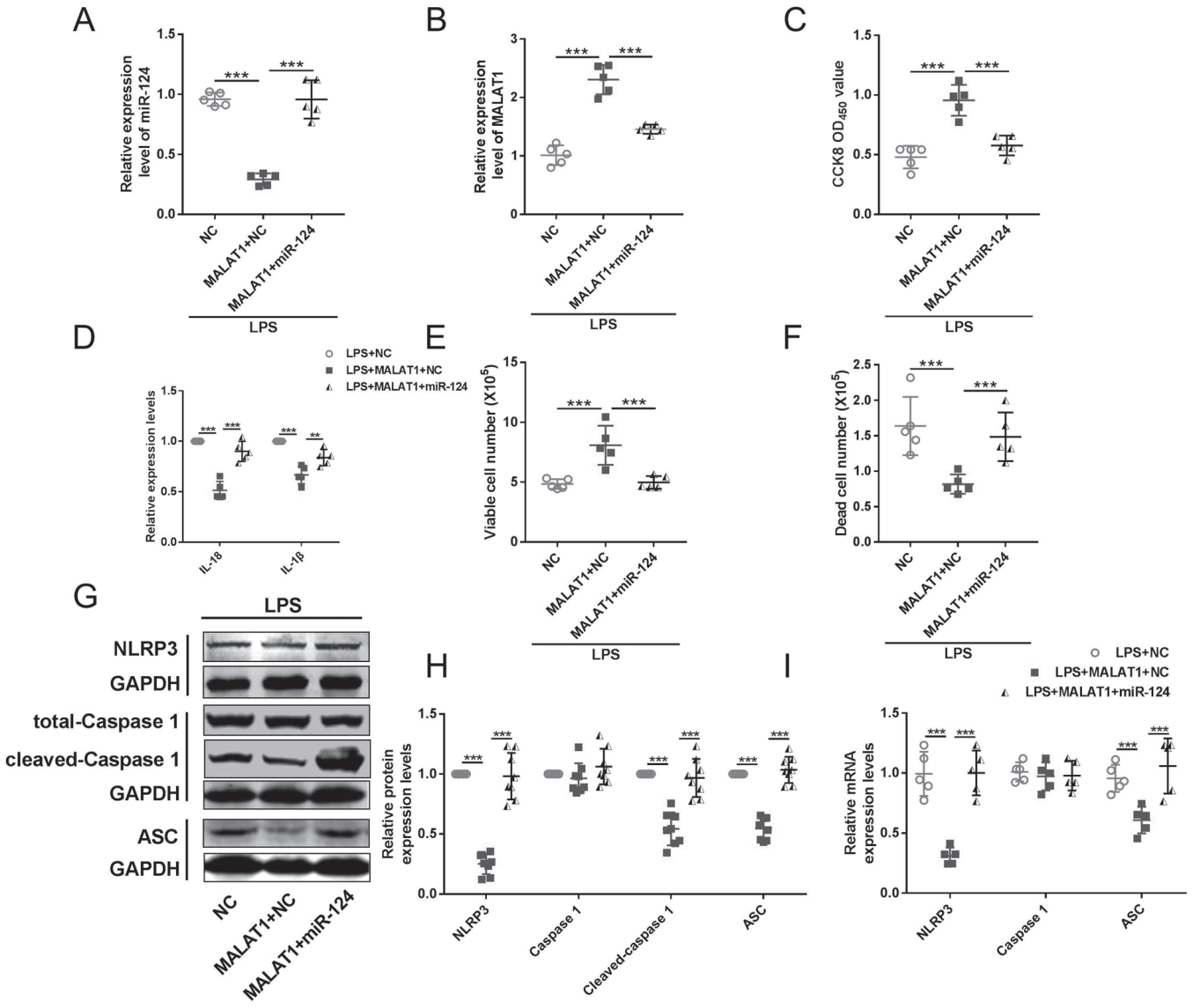

Figure 5. miR-124 mediates the regulation of lncRNA *MALAT1* on HeLa cervical cancer cell pyroptosis. RT-qPCR was performed to determine the expression levels of (A) miR-124 and (B) lncRNA *MALAT1* in LPS-treated HeLa cells. n=5; ***P<0.001. (C) Cell viability was detected by CCK-8 assay. n=5; ***P<0.001. (D) ELISA kits were used to determine the levels of IL-18 and IL-1β in the culture medium. n=5; **P<0.01, ***P<0.001. Trypan blue analysis was used to facilitate the detection of (E) viable and (F) dead cells. n=5; ***P<0.001. (G and H) Western blotting and (I) RT-qPCR were performed to detect the protein and mRNA expression levels, respectively, of pyroptotic factors, including NLRP3, caspase-1, cleaved caspase-1 and ASC. n=5; ***P<0.001. ASC, apoptosis-associated speck-like protein containing a caspase recruitment domain; CCK-8, Cell Counting Kit-8; lncRNA, long non-coding RNA; LPS, lipopolysaccharide; *MALAT1*, metastasis associated lung adenocarcinoma transcript 1; miR, microRNA; NLRP3, NOD-like receptor protein 3; OD, optical density; RT-qPCR, reverse transcription-quantitative PCR.

challenges, ongoing research is focused on developing promising treatments such as immunotherapies, targeted therapies, combination treatments, and genetic treatment approaches.

Gene targeted therapies have notable treatment effects, although limited effective targets and the difficulty in discovering new targets remain problematic. The basic requirements of therapeutic targets include: i) Significantly aberrant expression in carcinoma tissues compared with that in normal tissues; ii) association with cell viability, particularly proliferation and metastasis; and iii) their specific knockdown/knockout or overexpression must lead to a marked inhibition of cancer cell viability. Only factors exhibiting such characteristics should be considered as potential targets against cancer.

The present study focused on lncRNA *MALAT1* owing to its biological functions; according to GO analysis, the top two biological processes were 'regulation of cell proliferation' and 'regulation of cell cycle'. The positive relationship between lncRNA *MALAT1* and cell proliferation has been demonstrated in a number of cancer, fibroblast and smooth muscle cells with different downstream molecules (37-40). For example, lncRNA *MALAT1* promotes lung cancer cell proliferation as a miR-200a-specific sponge (18). Overexpression of lncRNA *MALAT1* enhances human periodontal ligament stem cell proliferation by regulating fibroblast growth factor 2 (41). lncRNA *MALAT1* impedes the proliferation of synoviocytes through β-catenin promoter methylation in rheumatoid arthritis (42). Based on these results, it was hypothesized that

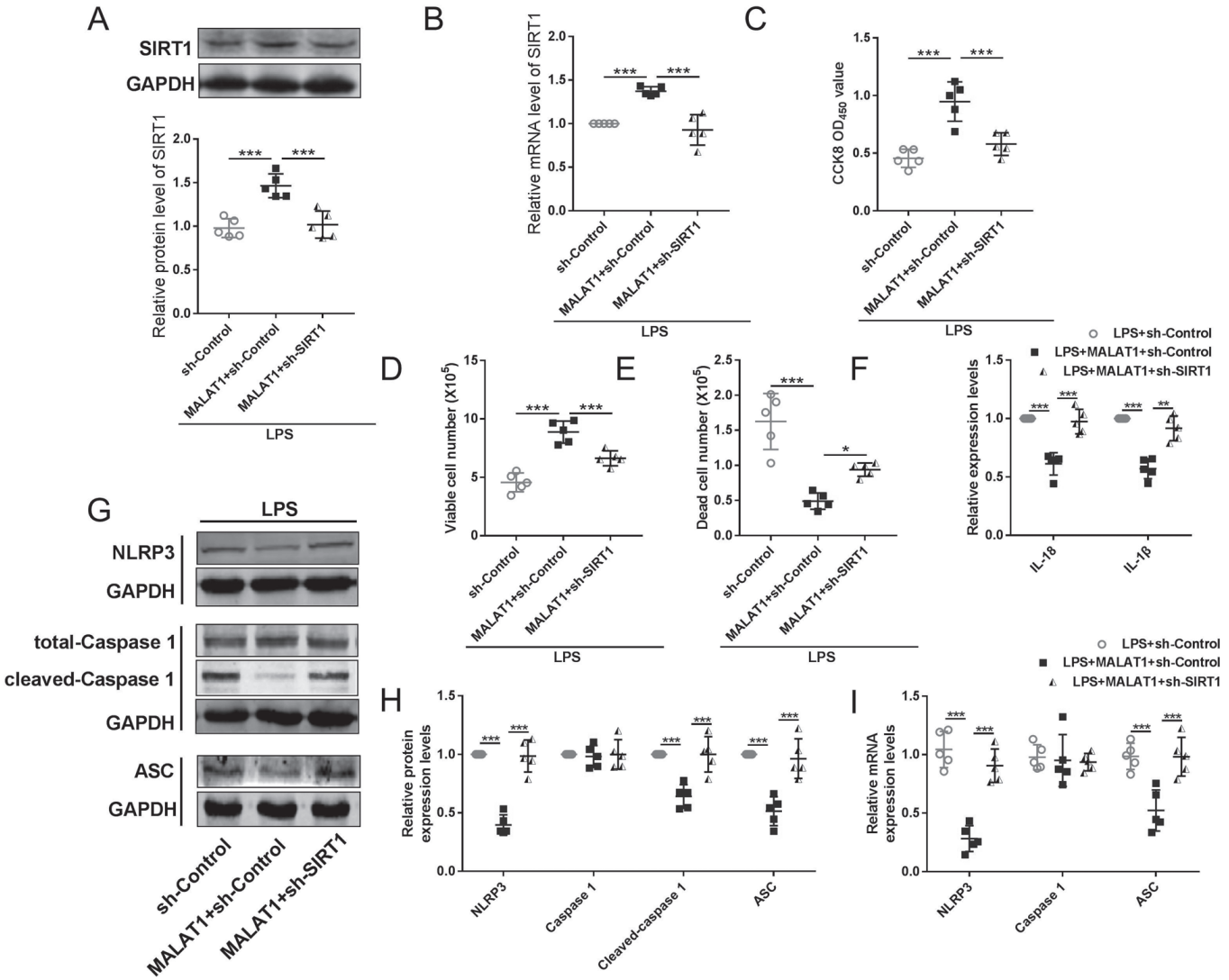

Figure 6. SIRT1 is a downstream effector of MALAT1 in HeLa cervical cancer cell pyroptosis. (A) Western blotting and (B) RT-qPCR were performed to determine the SIRT1 protein and mRNA expression levels, respectively, in LPS-treated HeLa cells. n=5; ***P<0.001. (C) Cell viability was detected by CCK-8 assay (n=5 in each group). ***P<0.001. (D) ELISA kits were used to determine the levels of IL-18 and IL-1β in the culture medium (n=5 in each group). ***P<0.001. (E and F) Cell numbers were detected by Trypan Blue analysis (n=5 in each group). *P<0.05, **P<0.01, ***P<0.001. (G-I) RT-qPCR and western blotting were performed to detect the mRNA and protein levels of pyroptotic factors, including NOD-like receptor protein 3, caspase-1, cleaved caspase-1 and apoptosis-associated speck-like protein containing a caspase recruitment domain (n=5). ***P<0.001. CCK-8, Cell Counting Kit-8; LPS, lipopolysaccharide; MALAT1, metastasis-associated lung adenocarcinoma transcript 1; OD, optical density; SIRT1, sirtuin 1; RT-qPCR, reverse transcription-quantitative PCR.

specific knockdown of lncRNA *MALAT1* could be a potential treatment against cell overproliferation-induced diseases. Previous studies indicated that knockdown of lncRNA *MALAT1* ameliorated osteoarthritis by promoting the apoptosis of chondrocytes (43). Furthermore, particularly in the progression of carcinoma, inhibition of lncRNA *MALAT1* showed markedly beneficial properties. For example, lncRNA *MALAT1* knockdown hinders prostate cancer progression by regulating the miR-140/baculoviral IAP repeat containing 6 axis (44) and inhibits cell proliferation by promoting the apoptosis of acute myeloid leukemia cells through the regulation of miR-96 (45). Previous studies also have reported that inhibiting lncRNA *MALAT1* protects low-*MALAT1*-expressing normal cells, including cardiomyocytes (46), podocytes (47), endothelial cells (48) and renal tubular epithelial cells (27), which is the opposite function to that observed in pathological tissues (such as carcinoma and atherosclerotic lesions), suggesting that lncRNA *MALAT1* may be a suitable therapeutic target. Therefore, the present study aimed to investigate the effects of lncRNA *MALAT1* on cervical cancer. Primary cervical cancer cells were isolated from carcinoma tissues, and a negative relationship between cell death and the expression of lncRNA *MALAT1* was observed; thus, the process of cell death was investigated in detail.

There has been an increased interest in pyroptosis over the past decade; however, studies focusing on pyroptosis still faces numerous limitations, particularly in the context of cancer development, which is complex and varies among species and organs (48). However, a previous study identified small molecule-mediated pyroptosis as an effective inhibitor of various tumor cells (49). Precise modulation of pyroptosis against intestinal tumors, inflammation or infectious disorders

in humans has been previously reported (50). lncRNA growth arrest specific 5 has been reported to suppress ovarian cancer by inducing pyroptosis (51). Knockdown of lncRNA X-inactive specific transcript inhibits the progression of NSCLC by targeting pyroptosis (52). lncRNA ADAM metallopeptidase with thrombospondin type 1 motif 9-antisense RNA 2 inhibits gastric cancer development by regulating the miR-223-3p/NLRP3 axis (53). Pyroptosis-targeted treatments may lead to a promising, novel approach to the treatment of patients with cancer. In the present study, upregulation of IL-18 and IL-1β was observed in the culture medium of cervical cancer cells, which suggested the involvement of pyroptosis of cervical cancer cells in lncRNA *MALAT1*-related cell death.

The present results revealed a negative association between lncRNA *MALAT1* and pyroptosis in cervical tumor cells, and overexpression of *MALAT1* blocked LPS-induced pyroptosis. In addition, it was observed that lncRNA *MALAT1* altered the levels of miR-124/SIRT1 in cervical cancer cells, and that the lncRNA *MALAT1*/miR-124/SIRT1 axis may regulate cervical cell pyroptosis, which, at least in part, was associated with tumor growth. Our findings provide a potential therapeutic strategy against cervical cancer by promoting pyroptosis.

The mechanism by which this regulatory axis is connected with pyroptotic factors was investigated in the present study. A previous study demonstrated the direct interaction between NLRP3 and p53 by chromatin immunoprecipitation analysis (21), and SIRT1 was reported to regulate the deacetylation of p53 (54). Whether specifically inactivating lncRNA *MALAT1* expression in cervical tumors using gene engineering tools could ameliorate the mortality and morbidity of cervical carcinoma, or other cancer types, thus providing more beneficial effects to improve the outcomes, requires further investigation.

In conclusion, lncRNA *MALAT1* may regulate pyroptosis through the miR-124/SIRT1 axis in cervical cancer cells. The present findings suggested that lncRNA *MALAT1* may be a potential target for improving the clinical effects of treatment in the progression of cervical carcinoma.

Acknowledgements

Not applicable.

Funding

The present study was supported by National Natural Science Foundation of China (82104173/82104169).

Availability of data and materials

The datasets used and/or analyzed during the current study are available from the corresponding author on reasonable request.

Authors' contributions

TL, DX and GZ contributed to the conception of the study. MJ, YW, YJ, SC, LD and XJ performed the experiment. TL and DX contributed significantly to analysis and manuscript preparation. GZ and DX performed the data analyses and wrote the manuscript. TL helped perform the analysis with constructive discussions. MJ, DX, GZ and YZ confirmed the authenticity of all the raw data. All authors have read and approved the final manuscript.

Ethics approval and consent to participate

Ethical approval was obtained from the Ethics Committee of The First Affiliated Hospital of Harbin Medical University (approval no. IRB-AF/SC-04/02.0; 11 November 2020). Tumor samples were collected from the patients upon written informed consent. The experimental protocols involving animals were approved by the Animal Ethical Care Committee of Qiqihar Medical University (approval no. QMU-AECC-2020-43; 8 May 2020) and complied with the Guide for the Use and Care of Laboratory Animals published by the USA National Institutes of Health (NIH Publication No. 85-23, revised 1996).

Patient consent for publication

Not applicable.

Competing interests

The authors declare that they have no competing interests.

References

1. Gu X, Sun G, Zheng R, Zhang S, Zeng H, Sun K, Wang S, Chen R and Wei W: Incidence and mortality of cervical cancer in China in 2015. J Natl Cancer Cent 2: 70-77, 2022.
2. Balasubramaniam SD, Balakrishnan V, Oon CE and Kaur G: Key molecular events in cervical cancer development. Medicina (Kaunas) 55: 384, 2019.
3. Barquet-Muñoz SA, Rendón-Pereira GJ, Acuña-González D, Peñate MV, Herrera-Montalvo LA, Gallardo-Alvarado LN, Cantú-de León DF and Pareja R: Role of pelvic and para-aortic lymphadenectomy in abandoned radical hysterectomy in cervical cancer. World J Surg Oncol 15: 23, 2017.
4. Bansal S, Lewin SN, Burke WM, Deutsch I, Sun X, Herzog TJ and Wright JD: Sarcoma of the cervix: Natural history and outcomes. Gynecol Oncol 118: 134-138, 2010.
5. Tang L, Liu S, Li S, Chen Y, Xie B and Zhou J: Induction mechanism of ferroptosis, necroptosis, and pyroptosis: A novel therapeutic target in nervous system diseases. Int J Mol Sci 24: 10127, 2023.
6. Zheng X, Chen W, Gong F, Chen Y and Chen E: The role and mechanism of pyroptosis and potential therapeutic targets in sepsis: A review. Front Immunol 12: 711939, 2021.
7. Kaczanowski S: Apoptosis: Its origin, history, maintenance and the medical implications for cancer and aging. Phys Biol 13: 031001, 2016.
8. Sun L, Ma W, Gao W, Xing Y, Chen L, Xia Z, Zhang Z and Dai Z: Propofol directly induces caspase-1-dependent macrophage pyroptosis through the NLRP3-ASC inflammasome. Cell Death Dis 10: 542, 2019.
9. Shen HH, Yang YX, Meng X, Luo XY, Li XM, Shuai ZW, Ye DQ and Pan HF: NLRP3: A promising therapeutic target for autoimmune diseases. Autoimmun Rev 17: 694-702, 2018.
10. Kovacs SB and Miao EA: Gasdermins: Effectors of pyroptosis. Trends Cell Biol 27: 673-684, 2017.
11. Xue Y, Enosi Tuipulotu D, Tan WH, Kay C and Man SM: Emerging activators and regulators of inflammasomes and pyroptosis. Trends Immunol 40: 1035-1052, 2019.
12. Varghese GP, Folkersen L, Strawbridge RJ, Halvorsen B, Yndestad A, Ranheim T, Krohg-Sørensen K, Skjelland M, Espevik T, Aukrust P, *et al*: NLRP3 inflammasome expression and activation in human atherosclerosis. J Am Heart Assoc 5: e003031, 2016.
13. Wang Y, Yin B, Li D, Wang G, Han X and Sun X: GSDME mediates caspase-3-dependent pyroptosis in gastric cancer. Biochem Biophys Res Commun 495: 1418-1425, 2017.

14. Fang Y, Tian S, Pan Y, Li W, Wang Q, Tang Y, Yu T, Wu X, Shi Y, Ma P and Shu Y: Pyroptosis: A new frontier in cancer. Biomed Pharmacother 121: 109595, 2020.
15. Qiao L, Wu X, Zhang J, Liu L, Sui X, Zhang R, Liu W, Shen F, Sun Y and Xi X: α-NETA induces pyroptosis of epithelial ovarian cancer cells through the GSDMD/caspase-4 pathway. FASEB J 33: 12760-12767, 2019.
16. Webb K, Prakash V, Kirresh O and Stewart A: A case of aortitis during cisplatin-based chemotherapy for cervical cancer. BJR Case Rep 5: 20180054, 2018.
17. Yang G, Lu X and Yuan L: LncRNA: A link between RNA and cancer. Biochim Biophys Acta 1839: 1097-1109, 2014.
18. Tseng YY, Moriarity BS, Gong W, Akiyama R, Tiwari A, Kawakami H, Ronning P, Reuland B, Guenther K, Beadnell TC, *et al*: PVT1 dependence in cancer with MYC copy-number increase. Nature 512: 82-86, 2014.
19. Kim J, Piao HL, Kim BJ, Yao F, Han Z, Wang Y, Xiao Z, Siverly AN, Lawhon SE, Ton BN, *et al*: Long noncoding RNA MALAT1 suppresses breast cancer metastasis. Nat Genet 50: 1705-1715, 2018.
20. Xu Y, Zhang X, Hu X, Zhou W, Zhang P, Zhang J, Yang S and Liu Y: The effects of lncRNA MALAT1 on proliferation, invasion and migration in colorectal cancer through regulating SOX9. Mol Med 24: 52, 2018.
21. Jin Y, Feng SJ, Qiu S, Shao N and Zheng JH: LncRNA MALAT1 promotes proliferation and metastasis in epithelial ovarian cancer via the PI3K-AKT pathway. Eur Rev Med Pharmacol Sci 21: 3176-3184, 2017.
22. Lin N, Yao Z, Xu M, Chen J, Lu Y, Yuan L, Zhou S, Zou X and Xu R: Long noncoding RNA MALAT1 potentiates growth and inhibits senescence by antagonizing ABI3BP in gallbladder cancer cells. J Exp Clin Cancer Res 38: 244, 2019.
23. Wu Q, Meng WY, Jie Y and Zhao H: LncRNA MALAT1 induces colon cancer development by regulating miR-129-5p/HMGB1 axis. J Cell Physiol 233: 6750-6757, 2018.
24. Feng C, Zhao Y, Li Y, Zhang T, Ma Y and Liu Y: LncRNA MALAT1 promotes lung cancer proliferation and gefitinib resistance by acting as a miR-200a sponge. Arch Bronconeumol (Engl Ed) 55: 627-633, 2019 (In English, Spanish).
25. Shi B, Wang Y and Yin F: MALAT1/miR-124/Capn4 axis regulates proliferation, invasion and EMT in nasopharyngeal carcinoma cells. Cancer Biol Ther 18: 792-800, 2017.
26. Zhang J, Jiang T, Liang X, Shu S, Xiang X, Zhang W, Guo T, Xie W, Deng W and Tang X: lncRNA MALAT1 mediated high glucose-induced HK-2 cell epithelial-to-mesenchymal transition and injury. J Physiol Biochem 75: 443-452, 2019.
27. Liu C, Zhuo H, Ye MY, Huang GX, Fan M and Huang XZ: LncRNA MALAT1 promoted high glucose-induced pyroptosis of renal tubular epithelial cell by sponging miR-30c targeting for NLRP3. Kaohsiung J Med Sci 36: 682-691, 2020.
28. Broutier L, Mastrogiovanni G, Verstegen MM, Francies HE, Gavarró LM, Bradshaw CR, Allen GE, Arnes-Benito R, Sidorova O, Gaspersz MP, *et al*: Human primary liver cancer-derived organoid cultures for disease modeling and drug screening. Nat Med 23: 1424-1435, 2017.
29. Qiu Z, He Y, Ming H, Lei S, Leng Y and Xia ZY: Lipopolysaccharide (LPS) aggravates high glucose- and hypoxia/reoxygenation-induced injury through activating ROS-dependent NLRP3 inflammasome-mediated pyroptosis in H9C2 cardiomyocytes. J Diabetes Res 2019: 8151836, 2019.
30. Kong M, Yao Y and Zhang H: Antitumor activity of enzymatically hydrolyzed Ganoderma lucidum polysaccharide on U14 cervical carcinoma-bearing mice. Int J Immunopathol Pharmacol 33: 2058738419869489, 2019.
31. Zhang T, Li Y, Zhu R, Song P, Wei Y, Liang T and Xu G: Transcription factor p53 suppresses tumor growth by prompting pyroptosis in non-small-cell lung cancer. Oxid Med Cell Longev 2019: 8746895, 2019.
32. So D, Shin HW, Kim J, Lee M, Myeong J, Chun YS and Park JW: Cervical cancer is addicted to SIRT1 disarming the AIM2 antiviral defense. Oncogene 37: 5191-5204, 2018.
33. Rerucha CM, Caro RJ and Wheeler VL: Cervical cancer screening. Am Fam Physician 97: 441-448, 2018.
34. Prince S: Cervical cancer treatments: Current challenges and future points of view. J Mol Oncol Res 6: 125, 2022.
35. PDQ Adult Treatment Editorial Board. Financial toxicity and cancer treatment (PDQ®): Health professional version. 2022 Sep 20. In: PDQ Cancer Information Summaries [Internet]. National Cancer Institute, Bethesda, MD, 2002.
36. Chao X, Song X, Wu H, You Y, Wu M and Li L: Selection of treatment regimens for recurrent cervical cancer. Front Oncol 11: 618485, 2021.
37. Lin L, Li Q, Hao W, Zhang Y, Zhao L and Han W: Upregulation of LncRNA Malat1 induced proliferation and migration of airway smooth muscle cells via miR-150-eIF4E/Akt signaling. Front Physiol 10: 1337, 2019.
38. Cooper DR, Wang C, Patel R, Trujillo A, Patel NA, Prather J, Gould LJ and Wu MH: Human adipose-derived stem cell conditioned media and exosomes containing MALAT1 promote human dermal fibroblast migration and ischemic wound healing. Adv Wound Care (New Rochelle) 7: 299-308, 2018.
39. Liao K, Lin Y, Gao W, Xiao Z, Medina R, Dmitriev P, Cui J, Zhuang Z, Zhao X, Qiu Y, *et al*: Blocking lncRNA MALAT1/miR-199a/ZHX1 axis inhibits glioblastoma proliferation and progression. Mol Ther Nucleic Acids 18: 388-399, 2019.
40. Liu J, Xu L and Zhan X: LncRNA MALAT1 regulates diabetic cardiac fibroblasts through the Hippo-YAP signaling pathway. Biochem Cell Biol 98: 537-547, 2020.
41. Chen P, Huang Y, Wang Y, Li S, Chu H and Rong M: MALAT1 overexpression promotes the proliferation of human periodontal ligament stem cells by upregulating fibroblast growth factor 2. Exp Ther Med 18: 1627-1632, 2019.
42. Li GQ, Fang YX, Liu Y, Meng FR, Wu X, Zhang CW, Zhang Y, Liu D and Gao B: MALAT1-driven inhibition of wnt signal impedes proliferation and inflammation in fibroblast-like synoviocytes through CTNNB1 promoter methylation in rheumatoid arthritis. Hum Gene Ther 30: 1008-1022, 2019.
43. Zhang Y, Wang F, Chen G, He R and Yang L: LncRNA MALAT1 promotes osteoarthritis by modulating miR-150-5p/AKT3 axis. Cell Biosci 9: 54, 2019.
44. Hao T, Wang Z, Yang J, Zhang Y, Shang Y and Sun J: MALAT1 knockdown inhibits prostate cancer progression by regulating miR-140/BIRC6 axis. Biomed Pharmacother 123: 109666, 2020.
45. Hu N, Chen L, Wang C and Zhao H: MALAT1 knockdown inhibits proliferation and enhances cytarabine chemosensitivity by upregulating miR-96 in acute myeloid leukemia cells. Biomed Pharmacother 112: 108720, 2019.
46. Wu A, Sun W and Mou F: lncRNA-MALAT1 promotes high glucose-induced H9C2 cardiomyocyte pyroptosis by downregulating miR-141-3p expression. Mol Med Rep 23: 259, 2021.
47. Zuo Y, Chen L, He X, Ye Z, Li L, Liu Z and Zhou S: Atorvastatin regulates MALAT1/miR-200c/NRF2 activity to protect against podocyte pyroptosis induced by high glucose. Diabetes Metab Syndr Obes 14: 1631-1645, 2021.
48. Song Y, Yang L, Guo R, Lu N, Shi Y and Wang X: Long noncoding RNA MALAT1 promotes high glucose-induced human endothelial cells pyroptosis by affecting NLRP3 expression through competitively binding miR-22. Biochem Biophys Res Commun 509: 359-366, 2019.
49. Ruan J, Wang S and Wang J: Mechanism and regulation of pyroptosis-mediated in cancer cell death. Chem Biol Interact 323: 109052, 2020.
50. Zhou CB and Fang JY: The role of pyroptosis in gastrointestinal cancer and immune responses to intestinal microbial infection. Biochim Biophys Acta Rev Cancer 1872: 1-10, 2019.
51. Li J, Yang C, Li Y, Chen A, Li L and You Z: LncRNA GAS5 suppresses ovarian cancer by inducing inflammasome formation. Biosci Rep 38: BSR20171150, 2018.
52. Liu J, Yao L, Zhang M, Jiang J, Yang M and Wang Y: Downregulation of LncRNA-XIST inhibited development of non-small cell lung cancer by activating miR-335/SOD2/ROS signal pathway mediated pyroptotic cell death. Aging (Albany NY) 11: 7830-7846, 2019.
53. Ren N, Jiang T, Wang C, Xie S, Xing Y, Piao D, Zhang T and Zhu Y: LncRNA ADAMTS9-AS2 inhibits gastric cancer (GC) development and sensitizes chemoresistant GC cells to cisplatin by regulating miR-223-3p/NLRP3 axis. Aging (Albany NY) 12: 11025-11041, 2020.
54. Chen H, Lin X, Yi X, Liu X, Yu R, Fan W, Ling Y, Liu Y and Xie W: SIRT1-mediated p53 deacetylation inhibits ferroptosis and alleviates heat stress-induced lung epithelial cells injury. Int J Hyperthermia 39: 977-986, 2022.